

# Enhanced ferromagnetism and magnetoelectric response in quenched BiFeO<sub>3</sub>-based ceramics\*

Qi Pan(潘祺) and Bao-Jin Chu(初宝进)<sup>†</sup>

Key Laboratory of Materials for Energy Conversion, Chinese Academy of Sciences (CAS), Department of Materials Science and Engineering, University of Science and Technology of China, Hefei 230026, China

(Received 28 March 2020; revised manuscript received 24 May 2020; accepted manuscript online 28 May 2020)

The piezoelectric, ferromagnetism, and magnetoelectric response of BiFeO<sub>3</sub>-BaTiO<sub>3</sub> ceramics with the compositions around the morphotropic phase boundary (MPB) of the solid solution are systematically investigated after the ceramics have been quenched from a high temperature. We find that the ferromagnetism of the quenched ceramics is greatly enhanced. An enhanced piezoelectric response  $d_{33}$  larger than 200 pC/N, which could be sustained up to 350 °C, is measured. As a result of enhanced ferromagnetism and piezoelectric response, a large magnetoelectric response  $\sim 1.3$  V/cm·Oe (1 Oe = 79.5775 A·m<sup>-1</sup>) is obtained near the mechanical resonance frequency of the quenched ceramic samples. Our research also shows that in addition to the ferromagnetism and piezoelectric response, the mechanical quality factor is another important parameter to achieve high magnetoelectric response because the physical effects are coupled through mechanical interaction in BiFeO<sub>3</sub>-based materials. Our work suggests that quenching is an effective approach to enhancing the magnetoelectric response of BiFeO<sub>3</sub>-based materials and the materials belong to single-phase multiferroic materials with high magnetoelectric response.

**Keywords:** multiferroic materials, magnetoelectric, ferromagnetic, piezoelectric

**PACS:** 75.85.+t, 76.50.+g, 77.55.H-

**DOI:** 10.1088/1674-1056/ab9736

## 1. Introduction

Multiferroic materials, in which ferroelectric orders coexist with ferromagnetic (or antiferromagnetic) orders, have been brought into focus due to their potential applications in sensors, transducers, and memories.<sup>[1,2]</sup> Different types of multiferroic materials have been studied in recent years, but many of the materials are not desirable for practical applications because the ferroelectric or ferromagnetic (or antiferromagnetic) order is often found at a temperature much below room temperature.<sup>[3-6]</sup> The BiFeO<sub>3</sub> (BFO) is one of the rare cases of multiferroic materials with both high Curie temperature  $T_c$  ( $\sim 825$  °C, for ferroelectric order)<sup>[7]</sup> and high Néel temperature ( $\sim 370$  °C, for the antiferromagnetic order).<sup>[8]</sup> However, BFO ceramics or thin film often exhibits large leakage, which affects the switching of ferroelectric polarization and the relevant functional properties, such as piezoelectric response.<sup>[9]</sup> In addition, although BFO possesses strong ferroelectricity, it is an antiferromagnetic (or weakly ferromagnetic) material.<sup>[10]</sup> Furthermore, the ferroelectric and antiferromagnetic (or ferromagnetic) orders in BFO originate from different microscopic mechanisms.<sup>[11]</sup> Due to these reasons, the magnetoelectric coupling effect of BFO is normally weak. Doping with aliovalent or isovalent ions, or forming solid solution with other ferroelectric compounds is an effective way to reduce the leakage and improve the ferroelectric or mag-

netic properties of BFO.<sup>[12-15]</sup> The solid solution of BFO and BaTiO<sub>3</sub> (BTO) is a typical material system, which has been intensively investigated. The solid solution of BFO with the appropriate amount of BTO was found to exhibit reduced conductivity, and enhanced ferroelectric or magnetic properties.<sup>[16]</sup> For example, it was found that the dielectric, ferroelectric and magnetoelectric properties were enhanced in BFO-BTO ceramics compared with BFO ceramics. It was also reported that Gd and Bi(Zn<sub>0.5</sub>Ti<sub>0.5</sub>)O<sub>3</sub>-modified BFO-BTO ceramics exhibited improved ferroelectricity.<sup>[17-19]</sup> The BFO and BTO have rhombohedral and tetragonal structures, respectively, and are similar to the observations in Pb(Zr,Ti)O<sub>3</sub> (PZT) solid solution.<sup>[20]</sup> A morphotropic phase boundary (MPB) emerges in the BFO-BTO solid solution. For the compositions near MPB, some physical properties of BFO-BTO ceramics, such as piezoelectric response, reach the maximum extents.<sup>[21]</sup> Due to this reason, the BFO-BTO ceramics has also been studied as high- $T_c$  lead-free piezoelectrics. In addition to the modification of compositions via doping or solid solution approach, processing has a significant effect on the physical properties of the BFO-based materials. Quenching the sintered BFO-based ceramics from a high temperature was found to reduce the conductivity and improve the ferroelectricity.<sup>[22,23]</sup>

The magnetoelectric (ME) response is the generation of electric polarization  $P$  (or magnetization  $M$ ) upon applying a

\*Project supported by the National Natural Science Foundation of China (Grant Nos. 51672261 and 51373161) and the National Key Research and Development Program of China (Grant No. 2017YFA0701301).

<sup>†</sup>Corresponding author. E-mail: chubj@ustc.edu.cn

magnetic field  $H$  (or electric field  $E$ ).<sup>[24–27]</sup> Like many multi-ferroic materials, the BFO-based materials have a weak ME response. An enhanced ME response at room temperature compared with BFO has been observed in BFO–BTO solid solution because of the improved ferroelectricity and ferromagnetism. The measured ME response in BFO–BTO thin film is typically around 0.1 V/cm·Oe.<sup>[28]</sup> Further doping of BFO–BTO ceramics can improve the ME response. For example, LaFeO<sub>3</sub> and La(Co<sub>0.5</sub>Mn<sub>0.5</sub>)O<sub>3</sub> modification of BFO–BTO ceramics enhances the ME response to  $\sim 0.67$  V/cm·Oe.<sup>[29,30]</sup> However, the ME response of BFO-based materials is still much weaker than that measured in magnetoelectric composites fabricated by magnetostrictive and piezoelectric materials, and the ME response of many composites can often be higher than 1 V/cm·Oe.<sup>[31–33]</sup>

Although the effect of quenching on the ferroelectric and piezoelectric properties of BFO-based materials are frequently studied, its effect on the ferromagnetism and ME response has seldom been reported. In this work, the piezoelectric response, ferromagnetism, and ME response of the quenched BFO–BTO ceramics with compositions near MPB are systematically investigated. We show that the quenching process not only improves the piezoelectric response, but also enhances ferromagnetism and ME response. A large ME response  $> 1$  V/cm·Oe is achieved in the BFO–BTO ceramics at mechanical resonance frequency. We also find that the highest ME response is not measured in compositions with the highest piezoelectric response nor with the strongest ferromagnetism. We propose that the mechanical quality factor should play an important role in generating the high ME response in BFO–BTO ceramics.

## 2. Experimental procedure

The  $(1-x)\text{BiFeO}_3-x\text{BaTiO}_3$  ( $(1-x)\text{BFO}-x\text{BTO}$ ) ceramic samples with the compositions in a range from  $x = 0.25$  to  $x = 0.4$  were prepared by using the conventional solid-state reaction method. The Bi<sub>2</sub>O<sub>3</sub> (purity 99.9%), BaCO<sub>3</sub> (purity 99.9%), Fe<sub>2</sub>O<sub>3</sub> (purity 99.9%), TiO<sub>2</sub> (purity 98.0%) were used as starting materials. All the raw materials are weighed according to stoichiometric ratio of the ceramics. Alcohol was added into the raw materials followed by ball milling. The mixture was calcined at 850 °C for 1 h and then at 940 °C for 1 h in sequence. The powder was pressed into disk samples by using polyvinyl alcohol as a binder. The wafers were heated at 600 °C for 3 h to remove the binder and then sintered at 1000 °C–1030 °C for 20 h. The sintered samples were abraded to a thickness of 0.4 mm by using sand paper. The abraded samples were treated at 850 °C for 30 min and then quickly quenched in the air. After being quenched, the ceramic wafers were cut into ceramic bars

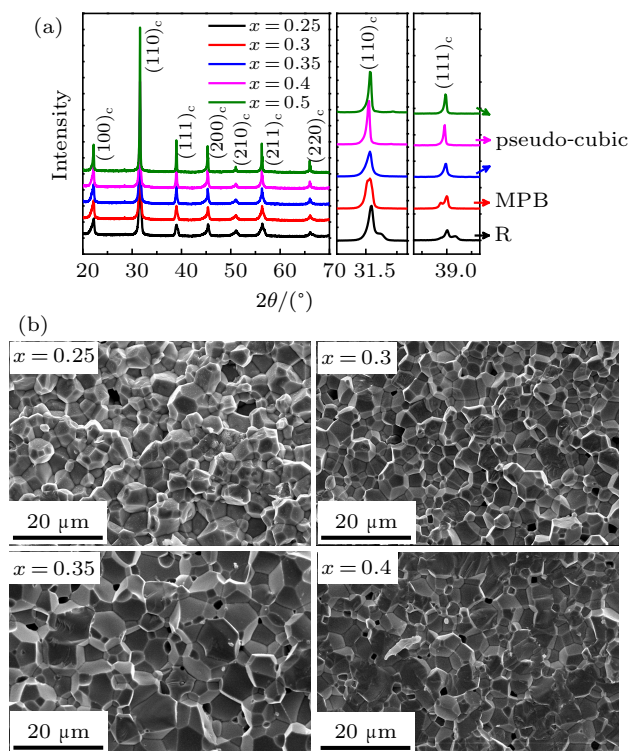
with the size of 20 mm×3 mm×0.4 mm by using a wire cutting machine (STX-202A, Kejing auto-instrument Co., Ltd., Shenyang). The crystal structures of  $(1-x)\text{BFO}-x\text{BTO}$  ceramics were measured by x-ray diffraction (XRD) through using Rigaku Smartlab diffractometer (Rigaku, Tokyo, Japan). The microstructure for each of the ceramic samples was examined by using a scanning electron microscope (SEM, Sirion200, FEI, USA).

Gold electrodes were deposited on the samples for electrical tests by using a sputter coater (EMS150T, Electron Microscopy Sciences, Hatfield, PA, USA). A quasi-static  $d_{33}$  meter (ZJ-6A, Institute of Acoustics, CAS, Beijing, China) was used to measure the piezoelectric coefficient  $d_{33}$  for each of the poled  $(1-x)\text{BFO}-x\text{BTO}$  samples. The poling process was performed at an electric field of 5 kV/mm at 120 °C for 15 min. The dielectric properties of  $(1-x)\text{BFO}-x\text{BTO}$  ceramics were measured by an LCR meter (model E4980, Agilent Technology, Santa Clara, CA, USA). The polarization–electric field ( $P$ – $E$ ) hysteresis loops were measured by using a modified Sawyer–Tower circuit (Polyktech, State College, USA). The vibrating sample magnetometer (SQUID-VSM, Quantum design, USA) was used to measure the magnetic hysteresis loops of  $(1-x)\text{BFO}-x\text{BTO}$  samples. The ME response was determined by a commercial ME measurement system (Super ME, Quantum design, USA). The magnetoelectric response of the BFO–BTO ceramics was measured by using the same procedure as that in Refs. [34,35]. During the measurement, a direct current (DC) magnetic field was applied to the ceramic samples. At the same time, a small AC magnetic field ( $< 2$  Oe) was applied to the samples to attain the magnetoelectric coefficient at this specific DC field. The DC magnetic field can be varied to obtain the coefficients under different DC fields. The impedance spectra of the poled  $(1-x)\text{BFO}-x\text{BTO}$  ceramic samples were measured by an impedance analyzer (4294A, Agilent, Santa Clara, CA) and the mechanical quality factor was obtained from the impedance spectra.<sup>[36]</sup>

## 3. Results and discussion

Figure 1(a) shows the XRD patterns of  $(1-x)\text{BFO}-x\text{BTO}$  ceramic samples with  $x$  in a range from 0.25 to 0.4. All the compositions have a perovskite structure without impurity phase according to the XRD patterns.<sup>[22]</sup> For BFO-based materials, (110) and (111) pseudocubic peaks have often been used to identify the phase structure, and in Fig. 1(a), the peaks are also shown.<sup>[37–39]</sup> The splitting of both (110) and (111) peaks, which indicates a rhombohedral (R) phase,<sup>[37]</sup> is observed in 0.75BFO–0.25BTO ceramics. A further increase in BTO content leads the crystal structure to transform from rhombohedral phase to pseudo-cubic phase. The 0.7BFO–0.3BTO ceramic has a structure with the features of both

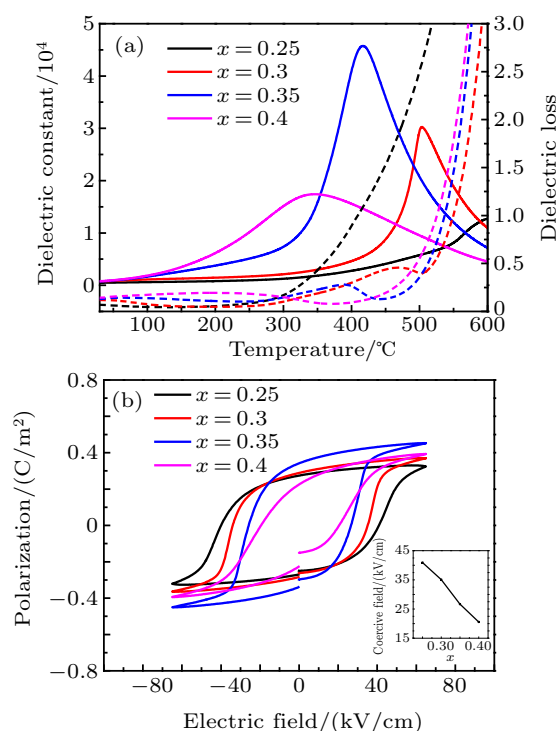
rhombohedral phase and pseudocubic phase, and the composition is thought to be near the rhombohedral–pseudo cubic (R–C) phase boundary. Figure 1(b) shows the cross-sectional SEM images of the  $(1-x)\text{BFO}-x\text{BTO}$  ceramic samples. All the compositions exhibit a dense microstructure and the ceramic grains have a well-defined shape. The grain size of the ceramics is in a range of  $5\ \mu\text{m}$ – $10\ \mu\text{m}$ .



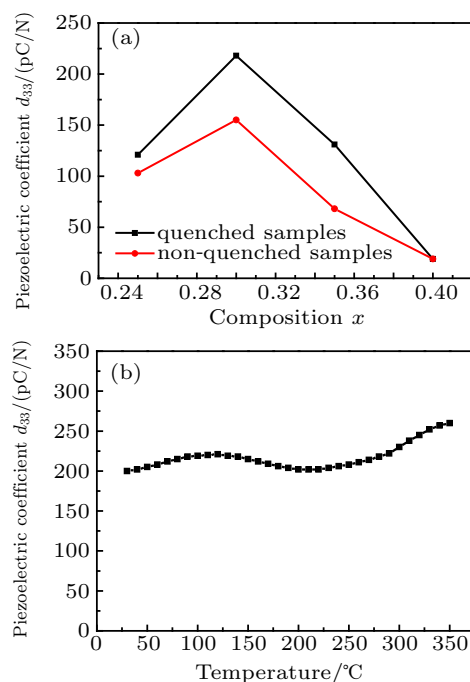
**Fig. 1.** (a) XRD patterns of  $(1-x)\text{BFO}-x\text{BTO}$  ceramic samples ( $x = 0.25$ – $0.4$ ), with two panels on the right showing (110) and (111) pseudo-cubic peaks, and (b) cross-sectional SEM images of  $(1-x)\text{BFO}-x\text{BTO}$  ceramic samples.

Figure 2(a) shows the temperature dependence of the weak-field dielectric constant and loss of  $(1-x)\text{BFO}-x\text{BTO}$  ceramic samples. The dielectric maximum temperature ( $T_m$ ) can be regarded as the Curie temperature of the material. Consistent with prior studies,  $T_m$  gradually moves to a lower temperature with the increase of BTO content, indicating the lowering of Curie temperature of the solid solution with more BTO content in the composition.<sup>[21,40]</sup> The dielectric loss of BFO–BTO ceramics is in a range from 0.07 to 0.14 below  $300\ ^\circ\text{C}$ . At a high temperature, the dielectric loss increases dramatically as a result of a high conduction or the contribution from other polarization mechanisms. The  $P$ – $E$  hysteresis loops of BFO–BTO ceramics are shown in Fig. 2(b). With the amount of BTO increasing, the coercive field of the ceramics decreases as shown in the inset of Fig. 2(b). When  $x$  is increased to 0.4, the ceramic exhibits a slim  $P$ – $E$  loop. It implies that the ferroelectricity is de-stabilized by the incorporation of BTO into the materials, and this result is consistent with the conclusion from XRD that the structure of the BFO–BTO ce-

ramics changes towards pseudocubic structure with BTO content increasing.



**Fig. 2.** (a) Temperature-dependent dielectric constants and dielectric losses of  $(1-x)\text{BFO}-x\text{BTO}$  ceramic samples (at 100 kHz), and (b)  $P$ – $E$  loops of  $(1-x)\text{BFO}-x\text{BTO}$  ceramic samples at room temperature (at 10 Hz), with inset showing coercive field varying with composition quantity.



**Fig. 3.** (a) Piezoelectric coefficient  $d_{33}$  versus composition of quenched and non-quenched BFO–BTO ceramics, and (b) temperature-dependent  $d_{33}$  of quenched 0.7BFO–0.3BTO ceramics from room temperature to  $350\ ^\circ\text{C}$ .

The piezoelectric response is an important parameter for generating the strong ME response. The variations of piezoelectric coefficient  $d_{33}$  with composition of the quenched BFO–BTO ceramics are shown in Fig. 3(a). Like the observation in PZT, the maximum  $d_{33}$  is measured to be  $215\ \text{pC/N}$  in

the quenched 0.7BFO–0.3BTO ceramics, a composition near the MPB of the solid solution. In Fig. 3(a), the piezoelectric response of the BFO–BTO ceramics without being subjected to the quenching process is also shown. Consistent with prior studies, the quenching process significantly enhances the piezoelectric response. From Fig. 2(a), we can see that the  $T_m$  of 0.7BFO–0.3BTO ceramics with the composition having the highest  $d_{33}$  among the BFO–BTO ceramics that we studied (Fig. 3(a)), is  $\sim 500$  °C, which is much higher than the  $T_c$  of PZT ceramics. It implies that the piezoelectric response of the ceramics can be sustained at a temperature much higher than that of the PZT ceramics. The temperature-dependent  $d_{33}$  of 0.7BFO–0.3BTO ceramics is measured and the result is shown in Fig. 3(b). The  $d_{33}$  of the ceramics is slightly dependent on the temperature below 350 °C, suggesting that BFO–BTO ceramics is a class of lead-free piezoelectric material with a high piezoelectric response, which promises to possess high-temperature applications.

Figure 4(a) shows the magnetic hysteresis ( $M$ – $H$ ) curves for the quenched  $(1-x)$ BFO– $x$ BTO ceramics with the compositions near the MPB. The changes of magnetization with magnetic field for four different compositions are shown in Fig. 4(a), where the inset displays the residual magnetization and coercive field varying with composition. The remnant magnetization increases first, reaching the maximum value when  $x = 0.3$ , and decreases then. The variation of magnetic properties with compositions can be attributed to the change of spiral modulated spin structure existing in BFO after incorporating BTO into BFO. The mechanism proposed for the observation of ferromagnetism in BFO–BTO solid solutions was reported in Ref. [16]. We notice that the magnetic properties in the quenched BFO–BTO ceramics are different from those reported in Ref. [16], which can be attributed to the difference in preparation conditions between the studies. Although the magnetic properties of BFO–BTO solid solutions have been widely studied, their magnetic responses in different reports<sup>[41–44]</sup> seem to be conflicting. Different factors, such as preparation conditions and stress could have a significant effect on magnetic response of BFO–BTO solid solution.<sup>[44,45]</sup> In our work, it is interesting that the composition is observed to be near the MPB ( $x = 0.3$ ), like other physical properties, such as piezoelectric response, the remnant magnetization reaches a maximum value.

Quenching is found to have a significant effect on the ferromagnetism of the BFO–BTO ceramics. Figure 4(b) shows  $M$ – $H$  curves for 0.7BFO–0.3BTO ceramics before and after quenching. An enhanced ferromagnetism is observed in air-quenched sample compared with the sample without being subjected to the quenching process. The remnant magnetization increases from 0.1263 emu/g to 0.2248 emu/g after quenching. The enhancement of ferromagnetism of the

quenched BFO–BTO is not clear and needs further studying. Because the stress enhanced ferromagnetism has been observed in BFO-based thin film,<sup>[45]</sup> we think, the quenching-induced internal stress in the materials could be one mechanism responsible for the enhancement in ferromagnetism of the 0.7BFO–0.3BTO ceramics. The stress may partly destruct the spin cycloid in BFO–BTO, resulting in the enhanced ferromagnetism in the quenched ceramics.

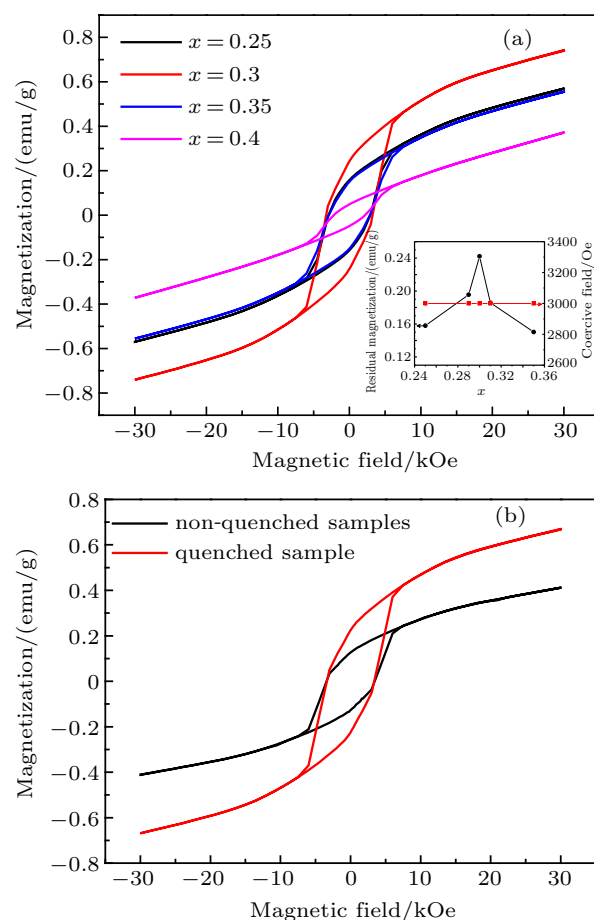


**Fig. 4.** (a) Magnetic hysteresis curves of quenched  $(1-x)$ BFO– $x$ BTO ceramics at room temperature for four different compositions, with inset displaying remnant magnetization and coercive field varying with composition of the ceramics. (b) Magnetic hysteresis curve of the quenched and non-quenched 0.7BFO–0.3BTO ceramics at room temperature.

The enhanced piezoelectric and magnetic properties in the quenched BFO–BTO ceramics result in an improved ME response. Figure 5(a) shows the curves of frequency-dependent magnetolectric coefficient ( $\alpha_{ME}$ ) of the quenched BFO–BTO rectangular ceramic bars at a DC magnetic field of 6000 Oe. During the ME measurement, the applied magnetic field is parallel to the surface of ceramic bars. As shown in Fig. 5(a),  $\alpha_{ME}$  peaks are observed to be in a frequency range between 70 kHz and 100 kHz for these four samples. The peaks are attributed to the excitation of the mechanical resonance in the BFO–BTO ceramics. In the inset of Fig. 5(a), the impedance spectra of 0.75BFO–0.25BTO ceramics are shown, and the resonance and antiresonance peaks originating from the longitudinal mechanical vibration of rectangular

ceramic plates through the transverse piezoelectric response ( $d_{31}$ ) can be observed. The frequencies for the maximum  $\alpha_{ME}$  are consistent with the resonance–antiresonance frequencies measured from the impedance spectra. From Fig. 5(a), it is interesting that the maximum ME response is observed in 0.75BFO–0.25BTO ceramics although the 0.7BFO–0.3BTO ceramics have the largest piezoelectric response (Fig. 3(a)) and the strongest ferromagnetism (Fig. 4(a)), the mechanism of which we will discuss later. A strong ME response  $\sim 1.3$  V/cm·Oe is measured near the resonance frequency of 0.75BFO–0.25BTO ceramic plate. The  $\alpha_{ME}$  of 0.6BFO–0.4BTO ceramics is negligibly small compared with those with other compositions because the  $d_{33}$  of the composition is small ( $\sim 19$  pC/N, Fig. 3(a)). The plots of dependence of the  $\alpha_{ME}$  of BFO–BTO ceramics at non-resonance frequency (10 kHz) on DC magnetic field for four different compositions are shown in Fig. 5(b). The  $\alpha_{ME}$  increases linearly with magnetic field increasing and is typically below 0.025 V/cm·Oe. From Figs. 5(a) and 5(b), we can see that the  $\alpha_{ME}$  at non-resonance frequency is much smaller than that measured at resonance frequency, reflecting the amplification of the ME response under mechanical resonance conditions.

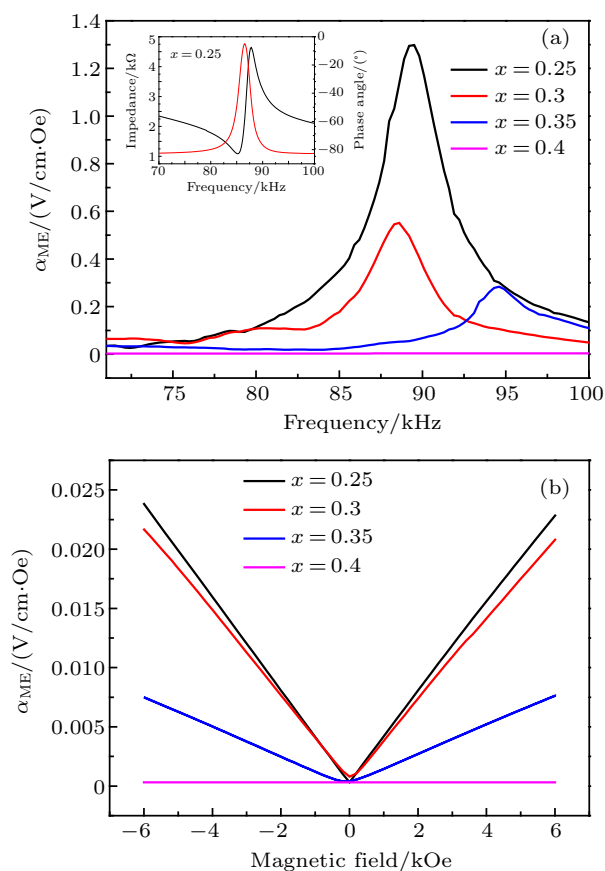


**Fig. 5.** (a) Frequency-dependent magneto-electric coupling coefficient  $\alpha_{ME}$  measured in  $(1-x)$ BFO– $x$ BTO ceramics with different compositions under a bias magnetic field of 6000 Oe, with inset displaying impedance spectrum and phase angle spectrum of the 0.75BFO–0.25BTO ceramics with  $x = 0.25$ . (b) Plots of magneto-electric coefficient ( $\alpha_{ME}$ ) versus bias magnetic field  $H_{bias}$  for  $(1-x)$ BFO– $x$ BTO ceramic samples with  $x = 0.25, 0.3, 0.35,$  and  $0.4$  (measured at 10 kHz).

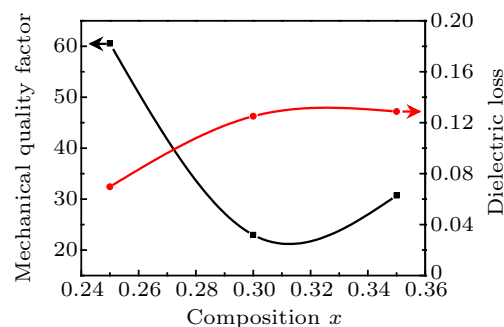


**Fig. 6.** Mechanical quality factor and dielectric loss versus composition of  $(1-x)$ BFO– $x$ BTO ceramics at room temperature.

Because the ferromagnetism and piezoelectric effect of BFO-based material originate from different microscopic mechanisms, the ME response is generated not from direct coupling of the two physical effects, but through the mechanical interaction. When  $\alpha_{ME}$  is measured, the mechanical response is first generated through the magneto-mechanical effect, which, we believe, is the magnetostriction because the sign of  $\alpha_{ME}$  does not change after the direction of the applied magnetic DC field has been reversed as shown in Fig. 5(b), and then converted into electrical response by the piezoelectric effect.<sup>[46]</sup> At mechanical resonance frequencies, the mechanical vibration can be amplified compared with that under the non-resonance state, and a parameter indicating the degree of the amplification is the mechanical quality factor  $Q_m$ . The  $Q_m$  of the BFO–BTO ceramics near MPB is determined from the impedance spectrum near the resonance–antiresonance frequency, a method that is often used in piezoelectric materials, and the results are shown in Fig. 6. Among the investigated compositions, 0.75BFO–0.25BTO ceramics has the highest  $Q_m$ . The  $Q_m$  decreases quickly when  $x > 0.28$ , reaches a minimum value at  $x = 0.32$ , and then increases slightly when  $x = 0.35$ . Since the 0.75BFO–0.25BTO ceramics has a much larger  $Q_m$  than those of other compositions, it is understandable that the ceramics exhibits the highest  $\alpha_{ME}$ . In fact, from Figs. 5 and 6 it follows that the product of the  $\alpha_{ME}$  measured at non-resonance frequency and  $Q_m$  is roughly equal to the  $\alpha_{ME}$  at resonance frequency, indicating that the large  $\alpha_{ME}$  of BFO–BTO at resonance frequency is mainly caused by the amplified mechanical vibration at resonance frequency. For example, the  $\alpha_{ME}$  of 0.75BFO–0.25BTO ceramics is  $\sim 0.024$  V/cm·Oe at 10 kHz under a DC magnetic field of 6000 Oe (Fig. 5(b)), and the  $Q_m$  is  $\sim 60$  (Fig. 6). The measured  $\alpha_{ME}$  at the resonance frequency under the same DC magnetic field is  $\sim 1.3$  V/(cm·Oe), which is close to the product of the  $\alpha_{ME}$  at non-resonance frequency and  $Q_m$ . In addition to  $Q_m$ , which is an indicator of the mechanical loss for mechanical vibration, BFO–BTO ceramics is a dielectric material, and dielectric loss may also be important for the high ME response. Among the investigated compositions, the 0.75BFO–0.25BTO

ceramics has the lowest dielectric loss, which is also desirable for a higher ME response as shown Fig. 6.

#### 4. Conclusions

In this work,  $(1-x)$ BFO- $x$ BTO ceramics with the compositions near the morphotropic phase boundary is prepared by using a conventional solid-state reaction method and the effect of quenching on the piezoelectric, magnetic, and magnetoelectric properties are investigated. We find that in addition to the piezoelectric response, the quenching of the ceramics from a high temperature can greatly enhance the ferromagnetism of BFO-BTO ceramics. A large piezoelectric response higher than 200 pC/N, which can be sustained at 350 °C, can be achieved in the quenched 0.7BFO-0.3BTO ceramics. Due to the high piezoelectric response and enhanced ferromagnetism of the quenched BFO-BTO ceramics, a greatly enhanced magnetoelectric response up to 1.30 V/cm-Oe is measured in 0.75BFO-0.25BTO ceramics at the mechanical resonance frequency of the sample. The mechanism for the composition dependence of the ME response is also investigated. We show that a high mechanical quality factor and low dielectric loss are desirable to achieve a high ME response, especially under the mechanical resonance conditions.

#### References

- [1] Khomskii D I 2006 *J. Magn. Magn. Mater.* **306** 1
- [2] Fiebig M, Lottermoser T, Frohlich D, Goltsev A V and Pisarev R V 2002 *Nature* **419** 818
- [3] Ravez J, Abrahams S C and Pape R D 1989 *J. Appl. Phys.* **65** 3987
- [4] Sarraute S, Ravez J, VonderMuhll R, Bravic G, Feigelson R S and Abrahams S C 1996 *Acta. Cryst. B.* **52** 72
- [5] Ravez J 1997 *J. Phys. III France* **7** 1129
- [6] Cheong S W and Mostovoy M 2007 *Nat. Mater.* **6** 13
- [7] Palai R, Katiyar R S, Schm H, Tissot P, Clark S J, Robertson J, Redfern S A T, Catalan G and Scott J F 2008 *Phys. Rev. B* **77** 014110
- [8] Catalan G and Scott J F 2009 *Adv. Mater.* **21** 2463
- [9] Qi X D, Dho J, Tomov R, Blamire M G and MacManus-Driscoll J L 2005 *Appl. Phys. Lett.* **86** 062903
- [10] Wang J, Neaton J B and Zheng H 2003 *Science* **299** 1719
- [11] Sharma P, Kumar A and Varshney D 2015 *Solid State Commun.* **220** 6
- [12] Kumara M and Yadav K L 2007 *Appl. Phys. Lett.* **91** 242901
- [13] Lee Y H, Wu J M and Lai C H 2006 *Appl. Phys. Lett.* **88** 042903
- [14] Kim J K, Kim S S and Kim W J 2006 *Appl. Phys. Lett.* **88** 132901
- [15] Yan T L, Chen B, Liu G, Niu R P, Shang J, Gao S, Xue W H, Jin J, Yang J R and Li R W 2017 *Chin. Phys. B* **26** 067702
- [16] Itoh N, Shimura T, Sakamoto W and Yogo T 2007 *Ferroelectrics* **356** 19
- [17] Zhang M, Zhang X Y, Qi X W, Li Y, Bao L and Gu Y H 2017 *Ceram. Int.* **43** 16957
- [18] Behera C and Pattanaik A K 2019 *J. Mater. Sci-Mater. El.* **089** 00140
- [19] Ryua G H, Hussaina A, Leea M H, Malik R A, Songa T K, Kim W J and Kim M H 2018 *J. Eur. Ceram. Soc.* **18** 30341
- [20] Du X H, Zheng J H, Belegundu U and Uchino K 1998 *Appl. Phys. Lett.* **72** 2421
- [21] Wei Y X, Wang X T, Zhu J T, Wang X L and Jia J J 2013 *J. Am. Ceram. Soc.* **96** 3163
- [22] Zhen T, Jiang Z G and Wu J G 2016 *Dalton Trans.* **45** 11277
- [23] Lee M H, Kim D J, Park J S, Kim S W, Song T K, Kim M H, Kim W J and Do D 2015 *Adv. Mater.* **27** 6976
- [24] He H, Zhao J T, Luo Z L, Yang Y J, Xu H, Hong B, Wang L X, Wang R X and Gao C 2016 *Chin. Phys. Lett.* **33** 67502
- [25] Zhao K H, Wang Y H, Shi X L, Liu N and Zhang L W 2015 *Chin. Phys. Lett.* **32** 87503
- [26] Rao W, Wang Y B, Wang Y A, Gao J X, Zhou W L and Yu J 2014 *Chin. Phys. Lett.* **31** 017503
- [27] Wang Y A, Wang Y B, Rao W, Gao J X, Zhou W L and Yu J 2013 *Chin. Phys. Lett.* **30** 047502
- [28] Gupta R, Shah J, Chaudhary S and Kotnala R K 2015 *J. Alloys Compd.* **638** 115
- [29] Luo L, Jiang N, Zou X, Shi D, Sun T, Zheng Q, Xu C G, Lam K H and Lin D M 2015 *Phys. Status Solidi A* **212** 2012
- [30] Zhang M, Zhang X Y, Qi X W, Zhu H G, Li Y and Gu Y H 2018 *Ceram. Int.* **44** 21269
- [31] Bichurin M I, Filippov D A and Petrov V M 2003 *Phys. Rev. B* **68** 132408
- [32] Filippov D A, Bichurin M I, Nan C W and Liu J M 2005 *J. Appl. Phys.* **97** 113910
- [33] Jia Y M, Luo H S, Zhao X Y and Wang F F 2008 *Adv. Mater.* **20** 4776
- [34] Pan Q, Fang C, Luo H S and Chu B J 2019 *J. Eur. Ceram. Soc.* **39** 1057
- [35] Pan Q and Chu B J 2019 *J. Appl. Phys.* **125** 154102
- [36] *IEEE Standard on Piezoelectricity*, ANSI/IEEE Std. 176-1987, IEEE, New York, 1987
- [37] Unruan S, Unruan M, Monnor T, Priya S and Yimnirun R 2015 *J. Am. Ceram. Soc.* **98** 3291
- [38] Kumar M M, Srinivas A and Suryanarayana S V 2000 *J. Appl. Phys.* **87** 855
- [39] Cao L, Zhou C R, Xu J W, Li Q L, Yuan C L and Chen G H 2016 *Phys. Status Solidi A* **213** 52
- [40] Wan Y, Li Y, Li Q, Zhou W, Zheng Q J, Wu X C, Zhu B P and Lin D M 2014 *J. Am. Ceram. Soc.* **97** 1809
- [41] Kumar M M, Srinath S, Kumar G S and Suryanarayana S V 1998 *J. Appl. Phys.* **188** 203
- [42] Wang T H, Ding Y, Tu C S, Yao Y D, Wu K T, Lin T C, Yu H H, Ku C S and Lee H Y 2011 *J. Appl. Phys.* **109** 07D907
- [43] Gotardo R A M, Viana D S F, Olzon-Dionysio M, Souza S D, Garcia D, Eiras J A, Alves M F S, Cotica L F, Santos I A and Coelho A A 2012 *J. Appl. Phys.* **112** 104112
- [44] Fujii T, Jinzenji S and Asahara Y 1988 *J. Appl. Phys.* **64** 5434
- [45] Bai F M, Wang J L, Wuttig M, Li J F, Wang N G, Pyatakov A P, Zvezdin A K, Cross L E and Viehland D 2005 *Appl. Phys. Lett.* **86** 032511
- [46] Ma J, Hu J M, Li Z and Nan C W 2011 *Adv. Mater.* **23** 1062